

The 13th International Fluid Power Conference, 13. IFK, March 21-23, 2022, Aachen, Germany

ENGINEERING
TOMORROW



Danfoss Digital Displacement & Editron: An efficient electro-hydraulic system for mobile applications

Jérémie Lagarde*, Matthew Green*, Alexis Dole*, Joonas Talvitie** and Juha Toikka**

Danfoss Scotland Ltd, Unit 3, Edgefield Industrial Estate, Loanhead, Midlothian, EH20 9TB, Scotland* Danfoss Editron, Laserkatu 6, 53850 Lappeenranta, Finland**

E-Mail: jeremie.lagarde@danfoss.com

Danfoss Digital Displacement & Editron: An efficient electro-hydraulic system for mobile applications

Despite the introduction of advanced battery electric mobile machines with zero CO₂ and tailpipe emissions, it is not until these machines are widespread that the environmental benefit will be felt. Currently the hydraulic systems required for low cost and robust linear actuation remain inefficient. This directly affects the required battery capacity, and the cost and operation time of the machines. In this paper, an electro-hydraulic system consisting of highly efficient components is tested to allow the creation of a validated loss model. The model is then used in combination with excavator operation data to show that the energy required to perform a typical day of operation, and therefore the capacity of the battery, can be reduced by 24.8%.

Keywords: Digital Displacement, Efficiency, Electrification, Hydraulics, Excavator

Target audience: Mobile Hydraulics, Electro-Hydraulics, Off-Highway Machinery

Future advances in Digital Displacement technology will allow for energy recovery and allow for further reductions in installed battery capacity.

With the urgency of climate change, emissions need to be reduced and alternative solutions for powering mobile construction machinery must be found.

1. INTRODUCTION

Off-highway equipment has been powered by diesel internal combustion engines (ICE) since the start of the 20th century and a significant shift from diesel is a huge challenge. However, with the urgency of climate change, emissions need to be reduced and alternative solutions for powering mobile construction machinery must be found.

With analytical support from the International Energy Agency, the Global Commission for Urgent Action on Energy Efficiency found that around 37% of the CO₂ emission reduction globally needs to come from an improvement in efficiency, while 32% should come from a switch to renewable energy [1]. The off-highway market is no exception, with conventional hydraulic systems showing an efficiency of 30 to 40% [2], [3]. Powered by a 40% efficient diesel engine [4], heavy equipment vehicles present an overall efficiency of less than 16%. In addition, tailpipe emissions of fine particulate matter and nitrogen dioxide have been identified as

a cause of poor public health [5].

Electric drives are well known to have a much higher efficiency than ICE and could be one way of reducing CO₂ emissions and eliminating local tailpipe emissions. They have been successfully implemented to replace conventional propel transmissions [6]; but, so far, have failed to replace hydraulic linear actuators. For reasons of cost, reliability and power density, hydraulic rams are still the preferred choice to generate linear movements and hydraulic systems are likely to stay in the heart of off-highway technologies for many years.

The use of electro-hydraulic systems in which the prime mover is an electric machine, but the actuation remains hydraulic, is common in stationary applications and a limited number of mobile applications, for example forklift trucks. For high power applications with limited or no access to an electricity network the cost of the associated energy source can be prohibitive. To achieve around 6 hours of operation the dealer Pon

Equipment install a 300kWh battery in the CAT320 Z-line excavator and report that this contributes considerably to the 3-fold price increase over the standard ICE driven machine [7]. Any improvement in system efficiency would of course reduce the energy requirement and therefore this cost.

The aim of this study is to understand the system efficiency benefit that the combination of a state-of-the-art electric machine and hydraulic machine could deliver. The efficiency of the components is tested to create validated loss models. The models are then used in a 1D simulation model of a 16 ton tracked excavator to compare the power requirement of different duty cycles and different system architectures employing these components. A baseline scenario using the loss model of a conventional swashplate machine is also simulated for comparison. The power requirements are then used to estimate the electrical energy required for a typical 8-hour shift. Finally, a breakdown of the system losses and the overall efficiency of the excavator is presented in Sankey diagrams.

2. SYSTEM UNDER TEST AND EXPERIMENTAL SETUP

2.1 Aim of the Test

The aim of the test is to measure the steady-state efficiency of the electro-hydraulic system shown in **Figure 1**.

The system is capable of converting direct current (DC) electrical power to hydraulic power. The test is also designed to measure the split in losses between the electric components and the hydraulic pump. For this reason, it is necessary to measure the electrical power, the hydraulic power, but also the mechanical rotational power. For completeness, the electrical power consumption of the pump controllers is also measured.

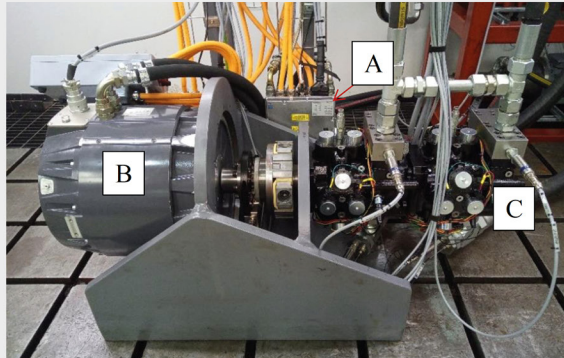


Figure 1: Photo of the system under test. A: electric converter, B: electric machine, C: hydraulic pump

2.1.1 Electric converter (EC)

An Editron C1200 converter is used as an inverter to control the rotational speed of the electric machine and has a switching frequency of 8kHz. It is sourcing its power from an active front end (AFE) which acts as a constant 700Vdc voltage source. While this voltage is high in comparison to that used in currently available electrified offhighway machines [8] it is expected that the off-highway market will follow the trend of increasing voltage that has been seen in the on-road sector, as evidenced by the voltage ratings of other electrification products.

2.1.2 Electric machine (EM)

The electric machine, operating as an electric motor, is based on synchronous reluctance assisted permanent magnet technology [9]. The model under test is from the PMI375 series and has dual windings for additional torque and power capabilities.

2.1.3 Hydraulic pump

The DDP096T hydraulic pump is a Digital Displacement® pump with a theoretical maximum displacement of 192cc/rev. It is a high-power, positive, and variable

displacement pump, with radially arranged pistons and electronically controlled valves [10]. The DDP096T pump is the tandem version of the DDP096, which means that it is two DDP096 pumps mounted front-to-back and mechanically coupled. For the hydraulic system, this means that there are two inlet and two outlet lines.

2.1.4 Pump controllers

The DPC12 controllers are embedded computers that control each mechatronic valve individually and can vary the pump displacement by choosing which piston to enable in real time. With a DDP096T pump, two DPC12 controllers are required to control all 24 valves. The controllers are setup in master/follower mode, which is the default configuration for tandem DDP096 pumps. The controllers are powered by a 24Vdc power supply.

2.2 Experimental setup

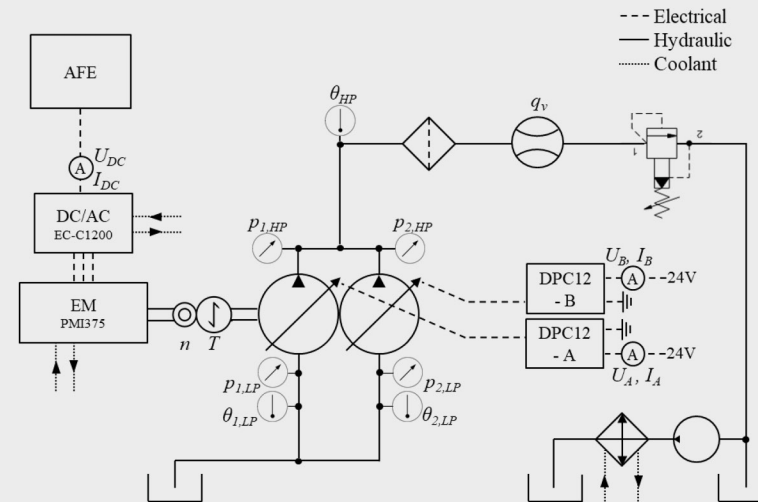


Figure 2: Simplified schematic of the hydraulic circuit used during the tests.

2.3 Measurement devices

Variables	Symbols	Sensor	Range	Accuracy
Shaft speed	n	HBM T40B	$\pm 20\,000$ rpm	1024 p/rev
Shaft torque	T	HBM T40B/1000	± 1000 Nm	0.04% FS
Low pressures	$p_{1,LP}, p_{2,LP}$	HBM P3ICP	0...20 bar	0.1% FS
High pressures	$p_{1,HP}, p_{2,HP}$	HBM P3ICP	0...500 bar	0.1% FS
Flow rate	q_v	VSE RS 400/10	1...400 L/min	0.5% MV
Temperatures	$\theta_{1,LP}, \theta_{2,LP}, \theta_{HP}$	PT100 1/10 DIN	-100...200 °C	0.13 °C
DC-Link Voltage	U_{DC}	LEM DVL 1000	± 1000 V	0.5% FS
DC-Link Current	DC-Link Current	LEM IT 605-S	± 600 A	0.0032% FS
DCP12 Voltage	DCP12 Voltage	Class A resistors	± 30 V	0.07% FS
DPC12 Current	DPC12 Current	PICO TA018	± 60 A	2.0% FS

Table 1: Instrumentation devices and their characteristics. Relative accuracy is given with respect to full scale (FS), measured value (MV), or actual units.

The sensors were connected to two synchronized DEWE-43A data acquisition units; except for the temperature sensors which were connected to Seneca ZC-4RTD units. The temperature readings were then broadcast via CAN bus and recorded by the DEWE-43 units.

According to ISO 4409:2019 [11], the shaft speed, flow rate, oil temperature and pressure measurements can be classified under class A in terms of their permissible systematic calibration errors. While most (88.7%) of the torque measurements fall under class A, few (8.5%) of them are under class B and very few (2.8%) under class C.

2.4 Range of requested steady-state operating points

To get an accurate representation of the performance of the electro-hydraulic system, a wide range of operating conditions were targeted:

Variables	Range	Unit
Outlet pressure	50, 100, 150, 200, 250, 300, 350, 400	bar
Shaft speed	750, 1000, 1250, 1500, 1750, 2000, 2250, 2500	rpm
Displacement fraction	25, 50, 75, 100	%
Oil temperature	50	°C
DC-Link Voltage	700	V

Table 2: Operating conditions of the system for the efficiency measurements

Due to the system and instrumentation limitations, some corners of the matrix of operating points could not be tested. For example, the flow meter’s maximum capacity of 400 L/min limited the shaft speed to 2000RPM when operating at 100% pump displacement.

The fluid used in the hydraulic circuit is Q8 Haydn 46 mineral hydraulic oil. This hydraulic oil is commonly used in many fluid power systems, both industrial and off-highway.

3 DEFINITIONS

3.1 Overall Efficiency and Losses

To determine the overall efficiency of the electro-hydraulic system, the input electric power P_{elec} and the output hydraulic power P_{hyd} first need to be defined.

ISO 4409:2019 standard does not give any guidance when it comes to testing a tandem pump with independently variable displacement front and rear pumps. One approach could be to consider the tandem pump as one single, big pump. But arguably, it is more accurate to look at the hydraulic power delivered by the front and the rear pump separately.

$$P_{elec} = U_{DC} \cdot I_{DC}$$

$$P_{hyd} = (q_{v1,HP} \cdot p_{1,HP} - q_{v1,LP} \cdot p_{1,LP}) + (p_{v2} \cdot p_{2,HP} - q_{vw,LP} \cdot p_{2,LP})$$

The DDP096T pump would not be able to output any flow without its DPC12 controllers, and therefore its associated electric power consumption P_{dpc12} should be accounted for.

$$P_{dpc12} = U_A \cdot I_A + U_B \cdot I_B$$

The overall efficiency of the system, η_{tot} , and overall power loss $P_{loss,tot}$ can now be defined as:

$$\eta_{tot} = \frac{P_{hyd}}{P_{elec} + P_{dpc12}}$$

$$P_{loss,tot} = P_{elec} + P_{dpc12} - P_{hyd}$$

3.2 Hydraulic Power Simplification

With un-boosted inlet lines, the hydraulic power of the fluid on the low-pressure side is very low and assuming that the inlet flow is equal to the outlet flow will result in negligible error. Equation (2) can now be simplified to:

$$P_{hyd} = q_{v1,HP} \cdot (p_{1,HP} - p_{1,LP}) + q_{v2,HP} \cdot (p_{2,HP} - p_{2,LP})$$

Equation (6) uses the respective outlet flow of the front and of the rear pump. However, with the presented experimental setup on **Figure 2**, the flow meter is measuring the total flow produced by the tandem pump. The digital nature of the DDP096T pump can however be used to estimate what proportion of the total flow is produced by which outlet. The DPC12 units control the pump's displacement fraction by adjusting the ratio of enabled cylinders versus disabled cylinders. Conveniently, the displacement fractions at which the DDP096T pump was tested produce fixed patterns of enabled cylinders, with the front and rear pumps using the exact same number of cylinders. The measured flow rate is therefore assumed to come equally from each outlet and the hydraulic power can be re-written as:

$$(1) \quad P_{hyd} = q_v \cdot (p_{HP} - p_{LP}) \quad (7)$$

$$(2) \quad \text{With,} \quad p_{HP} = \frac{p_{1,HP} + p_{2,HP}}{2} \quad (8)$$

$$(3) \quad p_{LP} = \frac{p_{1,LP} + p_{2,LP}}{2} \quad (9)$$

3.2.1 Note about the hydraulic power definition

The definition of the hydraulic power presented in Equation (2) does not account for the oil compressibility within the pump. A more accurate definition was proposed by Peter Achten et al. [12], although it is not yet recognized as the new standard calculation for hydraulic power and would result in higher efficiency values. In that respect, it can be said that the presented values are conservative.

3.3 Split of Power Losses

To differentiate between the losses of the electrical components and of the hydraulic pump, we need to calculate the mechanical rotational power P_{mech} :

$$P_{mech} = n \cdot T \quad (10)$$

The power loss of the combined electric converter and electric machine $P_{loss,ec+em}$ and the power loss of the DDP096T pump $P_{loss,ddp}$ are defined as follow:

$$(6) \quad P_{loss,ec+em} = P_{elec} - P_{mech} \quad (11)$$

$$P_{loss,ddp} = P_{mech} - P_{hyd} \quad (12)$$

4 TEST RESULTS

4.1 Overall efficiency results

Figure 3 presents the measured overall efficiency of the electro-hydraulic system, from inverter input power to pump hydraulic power, while also accounting for the DPC12 controller losses. The efficiency peaks at 89.0% efficiency, while being above 85% for most of the operating points where displacement fraction is greater than or equal to 50% (see Appendix A for details). In comparison, Ge et al. [13] measured a peak efficiency for their electro-hydraulic system of 71%. This was achieved using a frequency converter, an asynchronous electric motor, and a variable displacement electro-hydraulic axial piston pump.

Figure 3 shows that even with a pump displacement of 25%, the overall efficiency reaches 86.2% and most tested points are still above 80%.

4.2 Split in losses for a displacement fraction of 50%

Figure 4 presents a more detailed analysis of the losses for a displacement fraction of 50%. At this displacement, the peak efficiency is 88.5% and is reached at the maximum tested speed and pressure

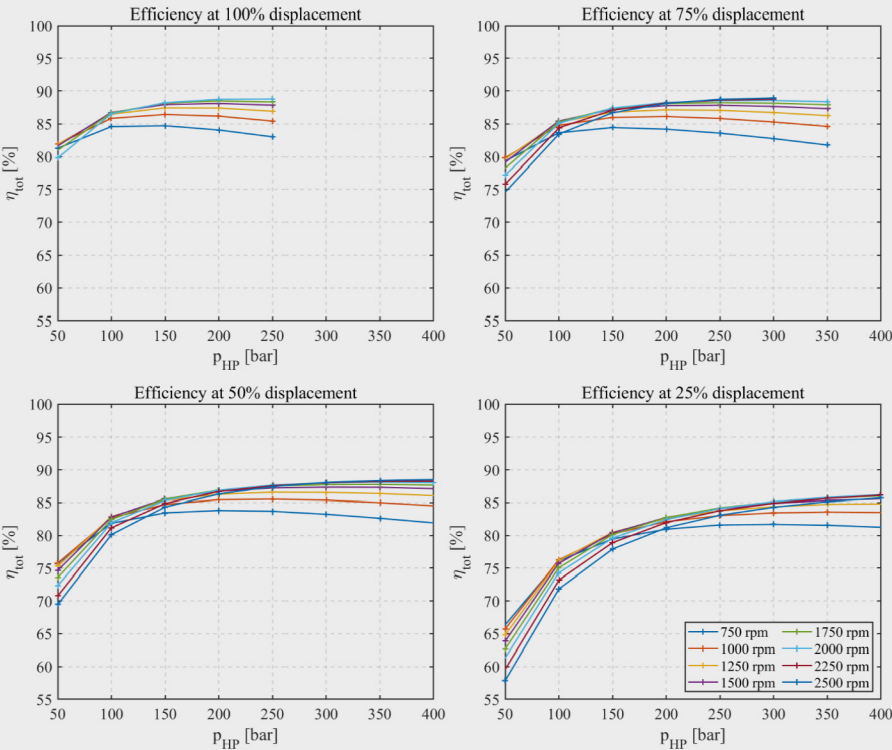


Figure 3: Overall efficiency results, measured at various displacement fractions.

(2500 rpm and 400 bar). It can also be noted that the overall efficiency stays above 85% for over 60% of the tested map. Figure 4 helps visualize the contributing loss of each component, and the trend they are following. The combined overall losses of the inverter and electric motor are, on average, slightly lower than those of the DD® pump. In fact, over the range of tested points, the EC + EM losses account for 46.7% of the losses, while the DDP096T pump contributes 50.9% and the DPC12 controllers only 2.4%.

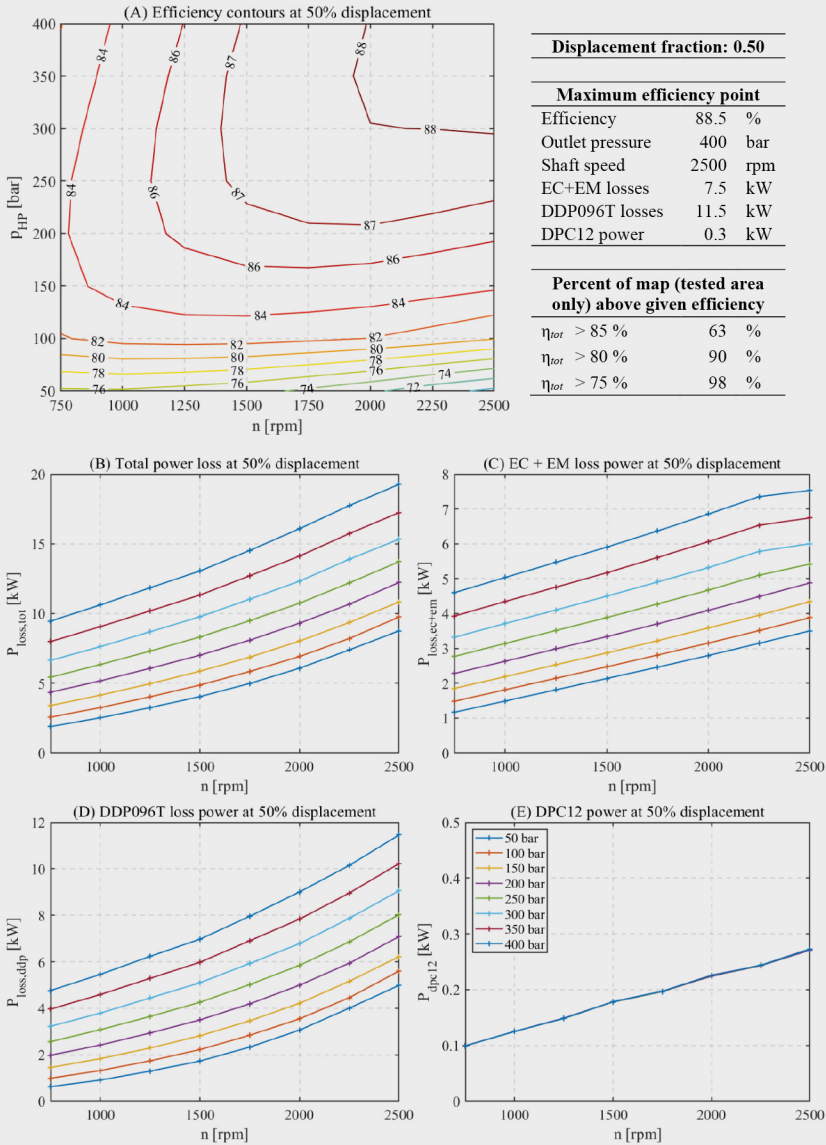


Figure 4: Contour map of the overall efficiency (A) and breakdown of the losses (B, C, D and E), at 50% displacement

5 LOSS MODELS

A loss model of the different components was created for the case study of a 16t tracked excavator.

5.1 Digital Displacement® pump loss model

The DDP096T pump loss model is based on the equations derived by Caldwell [14]. The model is semi-empirical with the pump losses being calculated from polynomial curves fitted to the measured data, while the flow and torque are calculated taking account of oil compressibility and pump geometry.

The model proposed by Caldwell was based on a different Digital Displacement® pump design which presented a linear increase in losses with respect to pressure, while the DDP096T pump’s losses are non-linear. The loss model was modified to account for this non-linearity.

As explained by Caldwell, the loss model takes advantages of the digital nature of the pump and calculates the losses as a proportion of the idle losses and of the losses at maximum displacement. The model presented in this paper was derived from the measured data at 50% displacement fraction, instead of 100% since more operating points could be tested at this partial displacement, resulting in more accurate curve fitting.

5.2 Pump controller loss model

The pump controllers’ power consumption is dominated by the electric power drawn by the solenoid valves and is, therefore, proportional to the frequency at which the solenoid valves are being actuated. This actuation

frequency is itself proportional to the displacement fraction and shaft speed.

5.3 Electric Converter and Machine Loss Model

The inverter and electric motor are modelled as one system, taking torque and shaft speed as inputs and outputting DC-Link voltage and current.

The test data shows that the voltage decreases very slightly (less than 2Vdc) and linearly as the torque increases, whilst the current increases following a 2nd order polynomial trend. These trends are also a function of shaft speed and, as a solution, the collection of polynomial coefficients are implemented as 1D look-up tables.

5.4 Analysis of the Models’ Accuracy

Figure 5 (A) shows how the different loss models interact with each other to calculate the required electric power from a set of shaft speed, outlet pressure and flow rate values. It also shows how the “Overall loss error (absolute)” was calculated to validate the accuracy of the loss models. Using the measured data, across the whole matrix of operating points, the maximum error is less than 0.4 kW. Figure 5 (B) presents a scatter representation of that error and shows that, in proportion to the input power, this overall loss error is less than 1.5%, while more than 90% of the points fall below 0.5% error. This is more than satisfactory for the purpose of the models.

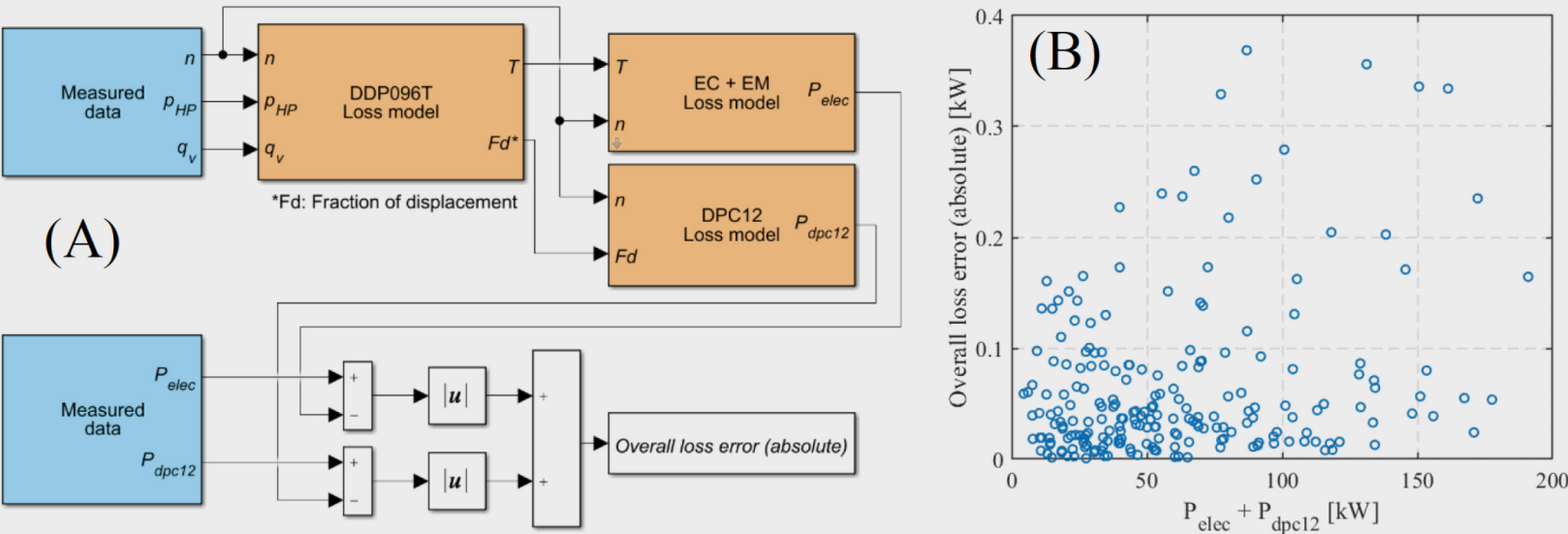


Figure 5: (A) Diagram of the loss models validation; (B) Scatter plot of the loss models’ overall loss error (abs.)

6 SIMULATION OF AN EXCAVATOR DUTY CYCLE

6.1 Duty cycle data description

To evaluate the performance of the combined system in an off-highway application, a 1D simulation was carried out in MATLAB Simulink using data recorded during duty cycle testing of a JCB JS160 tracked excavator. The excavator under test was equipped with a 93kW IC engine and a 2 x 96cc/rev Digital Displacement® pump [3]. The test data consists of 12 datasets of between 3 and 10 minutes duration, recorded during digging (including lorry loading and trenching), grading and tracking operations. Each dataset contains pressure and displacement for all functions (boom, bucket etc.), pump outlet pressure and flow, and prime mover shaft speed. The sampling rate is 10Hz.

6.2 Implementation of the electro-hydraulic system model

Table 3 details the hardware configurations that were simulated. The baseline, Case 1, was created by combining the Editron inverter and electric motor model created in the previous sections with a Kawasaki K3V [15] pump model, created following the method described by Dorey [16]. The Dorey loss

model of the K3V pump was created using test data from a 112cc/rev displacement pump. The displacement of the K3V is scaled down to match that of the DDP096T (2 x 96cc/rev). Cases 2 and 3 use the same inverter and electric motor model combined with the DDP096T pump model, as described in 5.15. System Architecture 1 (SA1) is typical of excavators of this size; two pumps provide flow to a main control valve (MCV) with two inlets, and the MCV can combine flow from both inlets to satisfy high flow demand functions [17]. System Architecture 2 (SA2) describes a system in which the main control valve has two inlets and two sets of spool valve but no ability to combine the inlets; high flow demand is satisfied by selectively increasing the pump displacement associated with each inlet, which is achieved using a Digital Displacement® pump with multiple outlets and an arrangement of switching valves. This configuration reduces

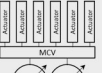
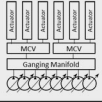
Case	Electric components	Hydraulic pump model	Hydraulic System Architecture
1: K3V SA1	Editron C1200 inverter and PMI375 electric motor	Kawasaki K3V 2 x 96 cc/rev	SA1 
2: DDP SA1		DDP096T 2 x 96 cc/rev	
3: DDP SA2		DDP096T 2 x 96 cc/rev	SA2 

Table 3: Presentation of the hardware configurations used in the duty cycle simulation

control valve losses as described in [18], increasing system efficiency.

6.3 Assumptions and limitations

The same PMI375 motor is used for all cases rather than applying a more conventional electric machine to the baseline case. Although efficiency data for an asynchronous motor as used for example by Ge et al [13] is available, it is unlikely that such a low power density and inefficient machine will be deployed in battery powered off-highway applications. A more appropriate comparison would be with another state-of-the-art motor (e.g. ABB AMXE), but efficiency models are not publicly available.

In all cases, the cooling system required to regulate the temperature of the electric motor, electric converter and hydraulic system is not included. It is expected that the power requirement of this system will be dramatically reduced compared to that in a conventional ICE driven system. In this study it is considered to be constant across the simulation cases and is neglected.

A pilot pump of 10cc/rev operating at 39bar is included in all cases and is given a fixed efficiency of 70% [17]. A DC/DC converter with a fixed efficiency of 80% is assumed to supply the electric power to the DPC12 controllers.

The pilot pump and the DC/DC power consumption are lumped together and described later as ‘additional load’.

The input voltage to the electric converter is assumed to be constant; no attempt to model the voltage characteristic of a battery has been made in this study. The additional 24Vdc control voltage supply to the inverter is neglected as it is <20W.

In all cases the prime mover speed percentage deviation from the mean is the same as the original ICE, with no dynamic speed adjustment. However, it is assumed that for the proportion of the time that an excavator is idle the prime mover speed is zero, and as a result the power requirement is zero. The relatively low inertia of the DDP096T, the high peak torque capability of the electric motor and therefore the ability to rapidly accelerate the shaft would enable this. In Case 1 it is not clear that this could be achieved, given the higher inertia of the K3V and the inability to operate at zero swash angle, but the same assumption of zero idle power requirement has been made.

In Case 1, it is assumed that the K3V torque and pressure limiting behaviour and frequency response matches that of the DDP096T, and as such it can deliver the required flow. In reality, the response time of the K3V is an order of magnitude higher, which in an ICE driven system reduces system efficiency by requiring a significant engine torque headroom to be maintained [3]. The effect of this on a system driven by an electric prime mover has not been studied.

In Case 3, the pump outlet pressure is modified to take into account the pressure drop of the additional switching valves and the reduction in main control valve pressure drop.

Finally, the backwards facing nature of the simulation means that no change in actuator trajectory or operator behaviour is accounted for. For example, increased actuator velocity resulting from reduced losses and therefore higher power to the actuator is not considered.

6.4 Simulation results

The average electric input power, *Pelec*, for each duty cycle and case is shown in Table 4.

The reduction in input power achieved in Case 2 is similar across all duty cycles and comes from a reduction in pump losses. But in Case 3, there is significantly more reduction for grading and digging, where multiple functions are operated simultaneously and the SA2 architecture is most beneficial. During travel, Case 3 offers no improvement over Case 2 since only one function is operational and there is no benefit to the SA2 architecture.

	Average input electric power, <i>Pelec</i> (kW) - [% reduction vs. Case 1]		
	Case 1: K3V SA1	Case 2: DDP SA1	Case 3: DDP SA2
Digging	60.8	57.1 [6.1%]	45.5 [25.1%]
Grading	62.6	59.4 [5.1%]	39.3 [37.3%]
Travel	63.6	60.8 [4.5%]	60.8 [4.5%]

Table 4: Average input electric power, for each case scenario and each duty cycle

In normal operation, an excavator performs a combination of these duty cycles. According to a study of 2015 [19], tracked excavators spend 60% of their time digging, while the remaining time is shared between grading (15%), travelling (10%) and idling (15%). Using these weighting coefficients, the energy consumption for a typical 8-hour day shift is calculated for each case scenario and presented in Figure 6. Cases 2 and 3 show respectively 5.7% and 24.8% reduction in

input energy compared to the baseline, Case 1. Neglecting battery efficiency and considerations such as dynamic behaviours, thermal effects, and state of charge, this means that Case 3 would require 24.8% less battery storage than Case 1; 314kWh instead of 418kWh. Clearly, different weighing coefficients would yield a different result, within the range 4.5% to 37.3% as shown in Table 4.

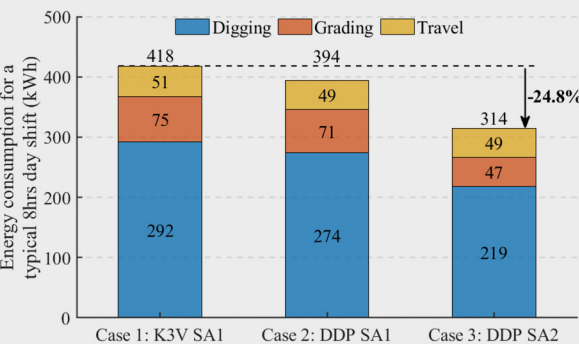


Figure 6: Weighted electric input energy of an 8-hour day shift for each case. Showing the percentage reduction with respect to Case 1.

With the weighting coefficients used in this study, the digging duty cycle accounts for most of the energy used. Figure 7 looks in detail at the different losses for that duty cycle, comparing the baseline Case 1 to Case 3. In both cases, the main source of losses is the MCV, but in Case 3 these losses

are reduced to almost half (from 23.4 to 12.9kW). Case 3 also shows lower pump losses since the DDP096T has significantly higher efficiency than the K3V pump. Finally, the additional losses of Case 3 are slightly higher than for Case 1 since the DPC12 losses are only included for the DDP cases. However, it is a relatively small increase (0.3kW).

The overall efficiency in Case 3 is 54.6%, compared to 40.9% in Case 1. Using an asynchronous machine would reduce the baseline efficiency further. [13] shows the peak combined efficiency of a frequency converter, asynchronous motor and swashplate pump to be 71%. Using Case 1 output power and MCV losses shown in Figure 7, this would result in an input power of 68.0kW and therefore a system efficiency of 36.6%.

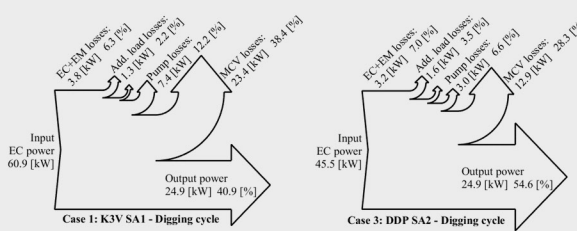


Figure 7: Sankey diagrams of the digging duty cycle, for the baseline K3V SA1 and DDP SA2 case scenarios

7 SUMMARY AND CONCLUSION


A state-of-the-art electro-hydraulic system, combining a Danfoss Editron inverter and electric motor with a Digital Displacement DDP096T pump and DPC12 pump controllers was tested so that a validated efficiency model of each component could be created. The test data shows a peak overall efficiency of 89.0%, from DC electric input power to pump hydraulic output power, while also accounting for the pump controller losses. For pump displacements of 50, 75 and 100%, most operating points show an efficiency of 85% and above. In fact, even with a pump displacement of 25%, the overall efficiency peaks at 86.2% and most tested points are above 80%.

Loss models of the inverter and electric motor combination (EC + EM), DDP096T pump and DPC12 controllers were made and validated based on experimental data. The validation shows an absolute error of less than 0.4kW, which in proportion to the input power, is less than 1.5% error.

These loss models were used to calculate the input energy required during typical operation of a 16 ton excavator,

using duty cycle data and a backwards facing simulation model. The results show that depending on the system complexity and the duty cycle weighting, a reduction in energy requirement of up to 24.8% is possible. This is achieved by using a DDP SA2 system (Case 3) which reduces pump and MCV losses. This system achieves an overall system efficiency of 54.6% during a digging operation. Neglecting battery considerations, a system based on Case 3 would require a 24.8% lower capacity battery than the baseline Case 1 to complete 8hrs of typical operation; 314kWh compared to 418 kWh

As part of further work, it would be interesting to investigate the benefits of efficiency optimization with respect to shaft speed. In fact, any given flow can be achieved by a range of speed/ displacement combination and the shaft speed used in the simulation model might not currently yield optimum efficiency results. In addition, to further increase system efficiency and reduce battery storage, the use of a Digital Displacement® pump/motor could be evaluated as it allows energy recovery [20].



To further increase system efficiency and reduce battery storage, the use of a Digital Displacement® pump/motor could be evaluated as it allows energy recovery.

ACKNOWLEDGEMENTS

The authors acknowledge the support of the Advanced Propulsion Centre who co-funded this work as part of the DDISPLACE project, and the technical contributions of David Logan, Marek Szupryczynski and Matteo Pellegri.

NOMENCLATURE

Variable	Description	Unit
n	Shaft speed	[1/s]
$p_{i,HP}$	Outlet pressure	[Pa]
$p_{i,LP}$	Inlet pressure	[Pa]
q_v	Flow rate	[m ³ /s]
P_{elec}	Electric power	[W]
P_{dpc12}	DPC12 controllers' power consumption	[W]
P_{hyd}	Hydraulic power	[W]
$P_{loss,ddp}$	Power loss of the DDP096T pump	[W]
$P_{loss,ec+em}$	Power loss of the electric converter and machine	[W]
$P_{loss,tot}$	Overall power loss	[W]
P_{mech}	Mechanical power	[W]
T	Shaft torque	[Nm]
θ_{HP}	Oil temperature in high pressure line	[K]
$\theta_{i,LP}$	Oil temperature in low pressure line	[K]
η_{tot}	Overall efficiency	[-]

REFERENCES

[1] Global Commission for Urgent Action on Energy Efficiency, "Recommendations of the Global Commission", 2020.

[2] L. Hoss, R. Bergstedt, J. Singh, R. Saha, D. Goyal and J. Potts, "Developing a portfolio of electrified powertrain options for off highway equipment", in 3rd TBM Forum for

Electrification & Battery Development for Non-road Applications., Frankfurt, Germany, 2020.

[3] M. Green, J. Macpherson, N. Caldwell and W. Rampen, "DEXTER: The Application of a Digital Displacement Pump to a 16 Tonne Excavator", in BATH/ASME 2018 Symposium on Fluid Power and Motion Control.

[4] Center for Alternative Fuels, Engines & Emissions - West Virginia University, "Heavy-Duty Vehicle Diesel Engine Efficiency Evaluation and Energy Audit", 2014.

[5] J. M. D. H. R. M. Susan Anenberg, "A Global Snapshot of the Air Pollution-Related Health Impacts of Transportation Sector Emissions in 2010 and 2015", International Council on Clean Transportation, Washington, 2019.

[6] Kramer, "The Kramer 5055e - in a vehicle class of its own", 28 10 2021. [Online]. Available: https://www.krameronline.com/fileadmin/user_upload/KC_EN_bro_5055e_KC.EMEA.10246.V03.EN_preview.pdf.

[7] M. Doyle, "Meeting Customer Demands, This Cat Dealer Opted to Produce Its Own Electric Excavator", 04 05 2021. [Online]. Available: <https://www.equipmentworld.com/technology/article/15065356/catdealer-produces-its-own-electric-excavator>.

[8] D. Beltrami, P. Iora, L. Tribioli and S. Uberti, "Electrification of Compact Off-Highway Vehicles—Overview of the Current State of the

Art and Trends", *Energies* 14(17), 2021.

[9] Danfoss, "Electric machines", [Online]. Available: <https://www.danfoss.com/en/products/dps/electricconverters-and-machines/electric-converters-and-machines/electric-machines/>. [Accessed: 07 01 2022].

[10] Danfoss, "Digital Displacement Pump Gen 2 Datasheet DDP096 and DPC12", 27 10 2021. [Online]. Available: <https://assets.danfoss.com/documents/163143/AI332064420016en-000104.pdf>.

[11] "ISO 4409:2019 Hydraulic fluid power -- Positive-displacement pumps, motors and integral transmissions -- Method of testing and presenting basic steady state performance", BSI Standards Publication.

[12] P. Achten, R. Mommers, T. Nishiumi, H. Murrenhoff, N. Sepehri, K. Stelson, J.-O. Palmberg and K. Schmitz, "Measuring the Losses of Hydrostatic Pumps and Motors - A critical Review of ISO4409:2007", in ASME/BATH 2019 - Symposium of Fluid Power and Motion Control, Sarasota, FL, USA, 2019.

[13] L. Ge, L. Quan, X. Zhang, Z. Dong und J. Yang, "Power Matching and Energy Efficiency Improvement of Hydraulic Excavator Driven With Speed and Displacement Variable Power Source", *Chinese Journal of Mechanical Engineering*, 2019.

[14] N. J. Caldwell, "Digital Displacement Hydrostatic Transmission Systems", Edinburgh, 2007.

[15] Kawasaki, 27 10 2021. [Online]. Available: https://global.kawasaki.com/en/industrial_equipment/hydraulic/pumps/pdf/k3v/k3vk5v_141016a.pdf.

[16] R. Dorey, "Modelling of losses in pumps and motors", in Proc. First Bath International Fluid Power Workshop, Bath, 1988.

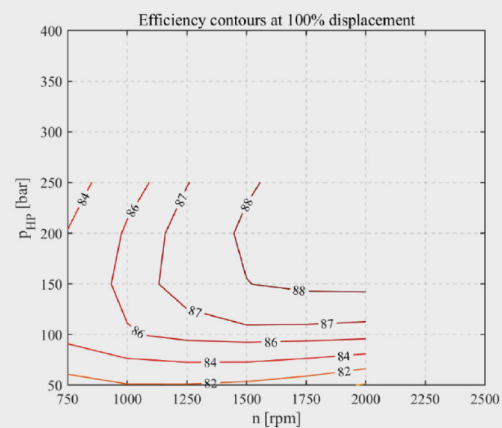
[17] KYB, "Hydraulic Components," 21 October 2021. [Online]. Available: www.kybfluidpower.com.

[18] M. Pellegri, M. Green, J. Macpherson, C. Mackay and N. Caldwell, "Applying a multi-service Digital Displacement Pump to an excavator to reduce valve losses", in 12th International Fluid Power Conference, Dresden, 2020.

[19] M. Helmus and M. Fecke, "Standardisierung definierter Lastzyklen und Messmethoden zur Energieverbrauchsermittlung von Baumaschinen : Schlussbericht zum Forschungsvorhaben", 2015.

[20] J. Hutcheson, D. Abrahams, M. Jill, N. Caldwell and W. Rampen, "Demonstration of Efficient Energy Recovery Systems Using Digital Displacement® Hydraulics", in 2020 Bath/ASME Symposium on Fluid Power and Motion Control FPMC2020, Bath, 2020.

APPENDIX A: EFFICIENCY CONTOUR
PLOTS AND SUMMARY TABLES

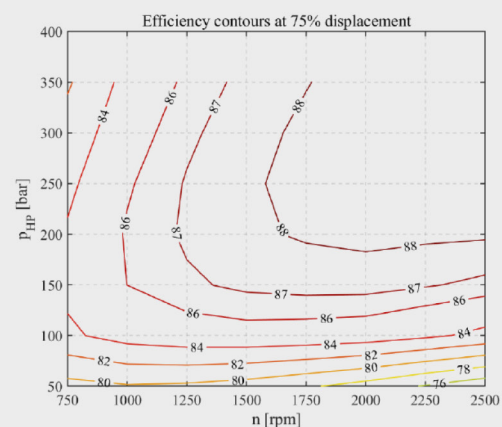


Displacement fraction: 100%

Maximum efficiency point	
Efficiency	88.8 %
Outlet pressure	250 bar
Shaft speed	2000 rpm
EC+EM losses	8.8 kW
DDP096T losses	9.8 kW
DPC12 power	0.4 kW

Percent of map (tested area only) above given efficiency

$\eta_{tot} > 85 \%$	76 %
$\eta_{tot} > 80 \%$	100 %
$\eta_{tot} > 75 \%$	100 %

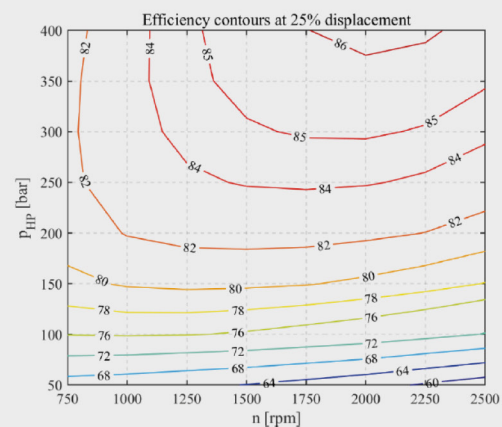


Displacement fraction: 75%

Maximum efficiency point	
Efficiency	89.0 %
Outlet pressure	300 bar
Shaft speed	2500 rpm
EC+EM losses	8.6 kW
DDP096T losses	12.0 kW
DPC12 power	0.4 kW

Percent of map (tested area only) above given efficiency

$\eta_{tot} > 85 \%$	75 %
$\eta_{tot} > 80 \%$	96 %
$\eta_{tot} > 75 \%$	100 %



Displacement fraction: 25%

Maximum efficiency point	
Efficiency	86.2 %
Outlet pressure	400 bar
Shaft speed	2000 rpm
EC+EM losses	4.0 kW
DDP096T losses	5.4 kW
DPC12 power	0.1 kW

Percent of map (tested area only) above given efficiency

$\eta_{tot} > 85 \%$	17 %
$\eta_{tot} > 80 \%$	70 %
$\eta_{tot} > 75 \%$	85 %